Improving the internal stress and wear resistance of DLC film by low content Ti doping

Li Qiang, Bin Zhang, Yan Zhou, Junyan Zhang*

State Key Laboratory of Solid Lubrication, Lanzhou Institute of Chemical Physics, Chinese Academy of Sciences, Lanzhou 730000, PR China

A R T I C L E   I N F O

A B S T R A C T

Low concentration Ti-doped hydrogenated amorphous carbon (Ti-C: H) films were deposited on silicon wafers by middle frequency magnetron sputtering titanium twin-targets in the feed gas of Ar/CH_4. Ti concentration was controlled by varying the gas flow ratio of Ar/CH_4 to be in the range of about 0.2—0.4 at.%. X-ray photoelectron spectroscopy (XPS), Raman and high-resolution transmission electron microscope (HRTEM) were used to analyze the composition and microstructure of the films. The internal stress, mechanical and tribological properties of the films were investigated by BGS 6341 type film stress tester, nanoindentation and reciprocating ball-on-disk tribo-tester, respectively. The results indicated that the incorporated Ti probably presents in the form of atomic state since no TiC was observed. The introduction of low content Ti significantly reduced the internal stress of DLC films with slight sacrifice of the hardness, and no obvious change was observed for the internal stress and hardness as the Ti content varies in the range of 0.2—0.42 at.%. Moreover, the low content Ti incorporation enhanced the friction and wear resistance of the DLC films dramatically with wear rate of $\sim 10^{-8}$ mm³/Nm and friction coefficient of 0.04. That is, no matter how much is Ti doping amount, the DLC film has excellent properties as long as the amount of Ti doping reaches the low content level.

1. Introduction

Diamond-like carbon (DLC) films have been investigated because of their promising properties such as high hardness, low friction coefficient, optical transparency and high chemical inertness [1]. Numerous techniques have been employed to deposit the DLC films: magnetron sputtering [2—5], filter cathodic vacuum arc [6,7], pulse laser deposition [8] and plasma enhanced chemical vapor deposition [9,10]. Among the above mentioned techniques, magnetron sputtering is the most suitable technique for large-scale industrial application.

Generally, however, there is high internal stress in DLC film, which restricts seriously the further application of DLC films. Because high stress would greatly weaken the adhesion strength of DLC films to substrates, resulting in the peeling off of the film from substrate during the deposition or in service. As an effective approach, metal doping, such as Ti, Cr, Al, W, Ni, has been proved to reduce internal stress and to increase the adhesion of DLC films

to substrates [11—16]. Active metals (like Ti, Cr, W, etc) would react with the carbon atoms of DLC films to form MeC carbide nanophase, and thus caused partial transformation of carbon hybridization from sp^3 to sp^2 [11,17—21], while chemical inert metals such as Al and Cu would present in atomic status. However, the internal stress was reduced as metal was incorporated into DLC film, but the weakened hardness came along too. It is reported that the hardness of DLC film reduced monotonically with increasing Cr content, because the formed CrC phase could break the continuity of the carbon network structure [13]. Moreover, some researches about Ti-doped DLC film have also been reported [22,23], We previously found that the incorporated Ti could present in atomic status in DLC film if the Ti content is very much low, which improved the mechanical and tribological properties of the DLC film significantly [24]. However, it will still lead to some of the thoughts: at low content, the change of Ti content is able to or not has a significant impact on the performance of film? Or the Ti content is lower, the better the performance of film? This paper is to answer the question. This is also the new ideal and purpose of this article! So more researches are required to verify the influence of low content Ti incorporation on the mechanical and tribological performance of DLC films, and whether there is significant difference or change as the content of Ti varies at the level of low concentration.

* Corresponding author. Tel.: +86 0931 4968295.
  E-mail addresses: qiangli1413@yahoo.cn (L. Qiang), zhangjunyan@licp.cas.cn (J. Zhang).

In present work, the Ti doping content is controlled at low concentration level to see if there is verify the influence of low content Ti incorporation on the mechanical and tribological performance of DLC films.

2. Experimental details

2.1. Films deposition

Different low concentration Ti-doped DLC films were prepared by magnetron sputtering system consisting of DC magnetron sputtering with 100 mm (W) × 672 mm (L) rectangular Ti twin-targets (99.99% purity). The doped titanium concentration was controlled by varying the gas flux ratio of Ar/CH$_4$. The volume of the vacuum chamber was 0.8 m^3. A n-type Si (100) wafer with the thickness of 625 ± 10 μm was used as the substrate. Prior to the deposition, all substrates were cleaned for 15 min using Ar$^+$ sputtering at the bias of −1200 V. Then, the vacuum chamber was evacuated up to 1.0×10^{-3} Pa. During films deposition, the working pressure was kept at a constant value of around 0.5 Pa through a pressure valve. CH$_4$ was introduced at 200 sccm into the chamber as the working gas. The power of the sputtering source was about 6.4 kW ($\sim$640 V, 10 A). A negative pulsed bias voltage of 1000 V was supplied during the films deposition. The deposition time was adjusted to obtain a film thickness of 2.0 ± 0.05 μm for all the samples. After deposition, the films were cooled down to room temperature inside the chamber. The Ti concentration in the DLC films increases from 0 to 0.21 at.% as the gas flux ratio of Ar/CH$_4$ from 0/200 to 40/200. Finally, the Ti concentration reaches to 0.42 at.% with the gas flux ratio of Ar/CH$_4$ increase to 80/200. The DLC films without Ti incorporation were prepared at the Ar/CH$_4$ ratio of 0/200 for the comparison. In the following text, the films with the Ti concentration of 0, 0.21, 0.30, 0.37 and 0.42 at.%, were denoted as pure DLC, Ti-DLC1, Ti-DLC2, Ti-DLC3, Ti-DLC4, respectively.

2.2. Sample characterization

The thickness of the DLC films was measured from the cross-section SEM images (Hitachi S-4800). A JEOL 2010 type high-resolution transmission electron microscope (HRTEM) operated at accelerating voltage of 200 kV was employed for microstructure characterization. The TEM samples with the thickness of 50 nm were first grown on NaCl wafers, and then the NaCl wafer was dissolved into the distilled water followed by placing the film onto Cu grids to obtain the TEM images. The chemical composition of the films was determined by VG ESCALAB 210 type X-ray photoelectron spectroscopy (XPS), with Al Kα radiation (photo energy 1476.6 eV) as the excitation source. Raman scattering was carried out with a LABRAM HR 800 Laser Raman spectroscopy with an excitation wavelength of 532 nm (2.34 eV). The mechanical properties were measured by nanoindentator (Nano indenter II, MTS, US). The indentation depth was controlled less than 10% of film thickness in order to avoid the influence of substrate. The internal stress was measured by BGS 6341 type Film Stress Tester. The tribological behaviors of the samples were investigated with a reciprocating ball-on-disc tester at 25 °C and relative humidity (RH) of 40%. Al$_2$O$_3$ with diameter of 5 mm was used as the counterface material. The sliding velocity was 10 cm s^{-1}, the applied load was 10 N, and the sliding length was 5 mm. All tests were performed at least five times to ensure the repeatability of the data. After testing, the wear volumes of the films were measured by a surface three-dimensional profiler, and then the specific wear rates were calculated by taking the volume of removed material over the load and the sliding distance.

3. Results and discussion

3.1. HRTEM analysis

Fig. 1 shows the HRTEM image and the corresponding selected area electron diffraction (SAED) pattern of the Ti-DLC4 film (0.42 at.% Ti). It can be seen that no special structure (like nano-crystalline, particulate) is observed in the film, the corresponding SAED also displays a diffuse halo without any diffraction ring, which clearly indicates the typical amorphous nature of diamond like carbon films, implying Ti might be dissolve in the DLC matrix in the form of atomic status.

3.2. XPS analysis

The X-ray photoelectron spectrometer (VG ESCALAB 210 type XPS) is employed to characterize the composition and the detail bonding state of the as-deposited films. Fig. 2(a) shows the XPS Ti 2p spectra of the Ti-DLC films with different low Ti concentration. All the Ti 2p spectra present two peaks at the binding energy about 458.8 eV and a shoulder peak at around 464.2 eV. The Ti concentration increases from 0 to 0.21 at.% as the gas flux ratio of Ar/CH$_4$ from 0/200 to 40/200. Finally, the Ti concentration reaches to 0.42 at.% with the gas flux ratio of Ar/CH$_4$ increase to 80/200. Actually, Ti 2p peak is unsuitable to differentiate the chemical bonds between Ti and TiC, because the binding energy of TiC (455 eV) and TiO (455.1 eV) is so close that it is hardly to be distinguished [12]. Nevertheless, the C1s XPS spectrum can be used to further confirm the absence of TiC phase. Fig. 2(b) illustrates the XPS C1s spectra of the films with different Ti concentration that no significant difference of the peak shapes is observed, while the binding energy of C1s shifts toward lower value as the Ti concentration increases from 0 to 0.42 at.%, which implies increased sp^2-hybridized carbon atoms content. The spectra can be deconvoluted into three Gaussian peaks with the binding energies at 281.7 eV for the Ti−C bonds [25], 284.6 eV for sp^2 hybrid carbon bonds, and 285.2 eV for sp^3 hybrid carbon bonds, respectively, if there is TiC in DLC films. Apparently, no peak at 281.7 eV (corresponding to the
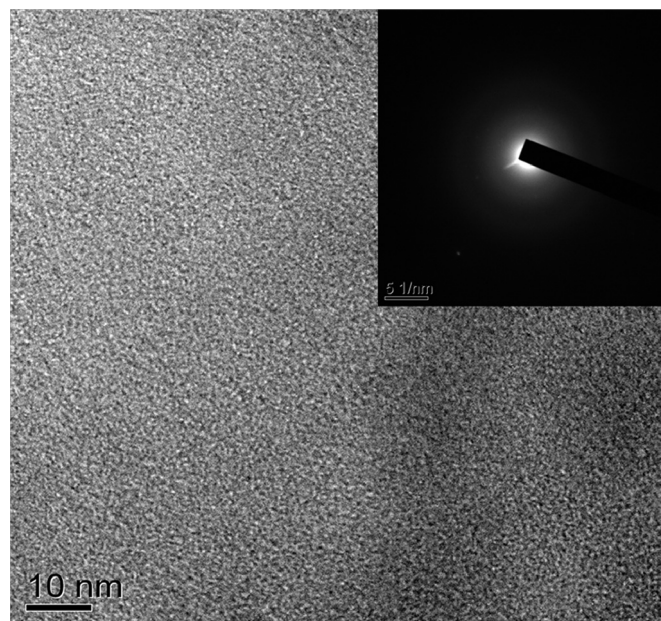

Fig. 1. The HRTEM image and the corresponding selected area electron diffraction (SAED) pattern of the Ti-DLC4 film (0.42 at.% Ti).
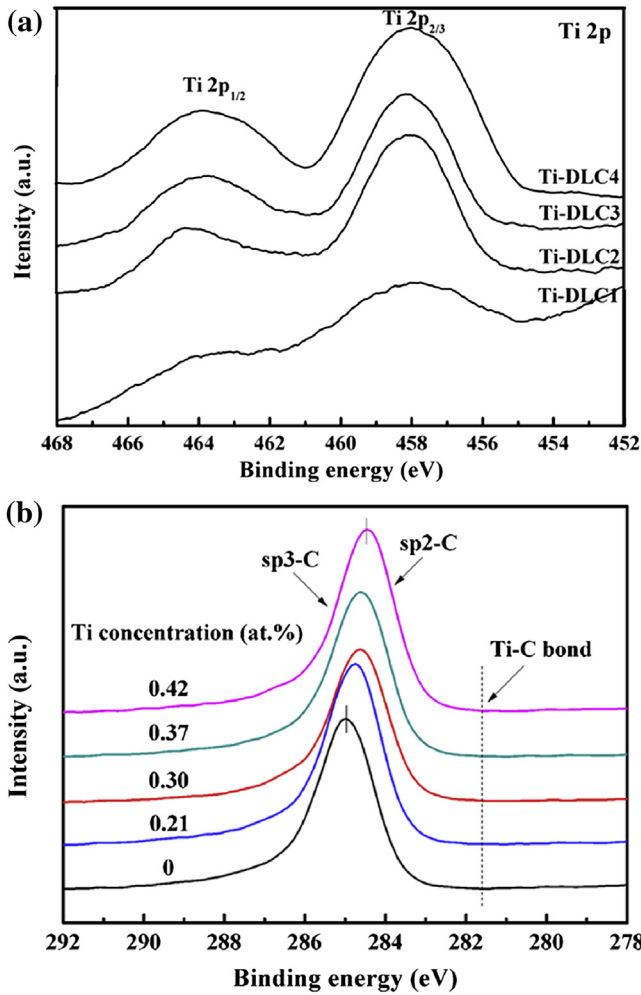
Fig. 2. (a) The Ti 2p and (b) C1s XPS spectra of the films as a function of the Ti concentration.

Fig. 3. The sp^3/sp^2 ratios as a function of the Ti concentration.

Ti–C bonds) could be found in the XPS spectra, which implies the Ti does not bond with carbon atom, is in good agreement with the HRTEM result. Generally, the sp^3 hybrid carbon controls the mechanical properties of DLC films, therefore, the relative proportion of sp^3 to sp^2 is a key factor to assess DLC films. The sp^3/sp^2 ratios of the DLC films were calculated by taking the ratio of the sp^3 peak area over the sp^2 peak area and the results obtained are shown in Fig. 3. The sp^3/sp^2 ratio has almost no obvious change with the increase in the Ti concentration, 0.41 for the pure DLC film, 0.37 for Ti-DLC1 film and 0.33 for Ti-DLC4 (0.42 at.% Ti) film, which directly demonstrates the sp^3 content has little change with the increasing of the Ti concentration.

3.3. Raman analysis

The XPS is employed to get quantitative results of the films composition (sp^3/sp^2 ratio). However, it is hardly applied to a very tiny area, while Raman spectroscopy, which is an effective and nondestructive tool, was used to characterize the detailed bonding structure of the Ti-DLC film using Ar^+ laser of 532 nm. Generally, the Raman spectrum of DLC film is consisted of two peaks in the range of 800 cm^{-1}–2000 cm^{-1}, the so-called G and D peaks located at around 1580 cm^{-1} and 1350 cm^{-1}, respectively [26]. The G bond is attributed to the symmetric E2g C–C stretching mode in graphite-like material, while the D bond is assigned to bond angle

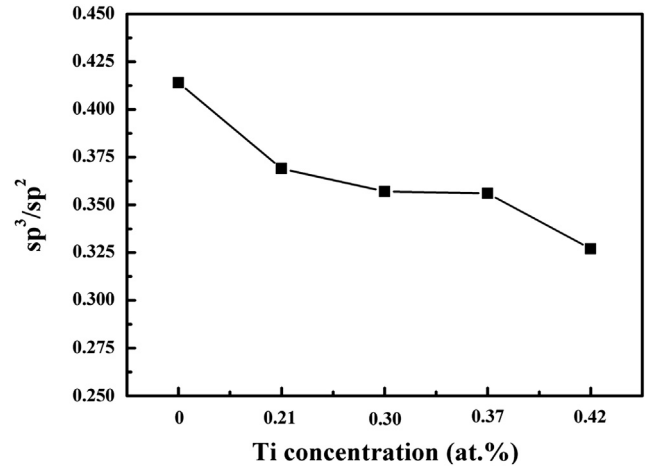disorder in the graphite-like microdomains [27]. Normally, the relative intensities ratio of the D and G bonds (I_D/I_G) and the G peak position could be used to characterize the sp^3/sp^2 ratio, and the I_D/I_G ratio increases with the increasing of sp^2 content in the hydrogenated amorphous DLC films [27].

Fig. 4(a) presents the Raman spectra of the films with different Ti concentrations. It is clear that the spectra have two bonds centered at 1350 cm^{-1} (D bond) and 1580 cm^{-1} (G bond), indicating a typical amorphous structure of the films. The G peak position and the I_D/I_G ratio as a function of the Ti concentration are shown in
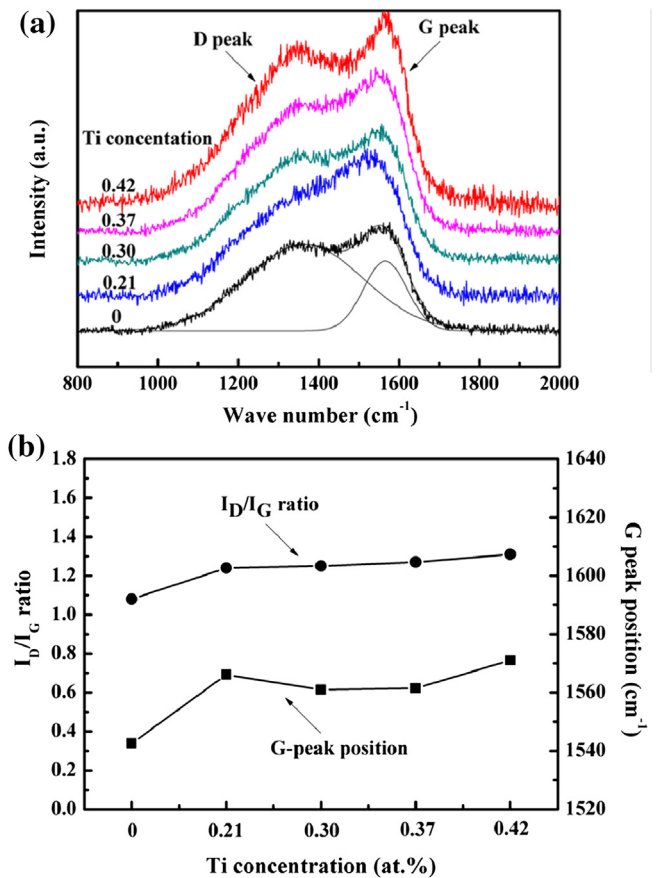

Fig. 4. (a) Raman spectra (b) the corresponding G peak position and I_D/I_G ratio of the Ti-DLC films with the different Ti concentration.

Fig. 4(b). It should be noted that the I_D/I_G ratio almost keeps at a constant value of 1.27 ± 0.04, while the G peak position of the films only also shift from 1566.12 cm^{-1} to 1571 cm^{-1}, this indicated that the sp^3 content has little change with the increasing of the Ti concentration, which is well consistent with the XPS results.

3.4. Internal stress and hardness

Fig. 5 shows the internal stress, hardness and elastic modulus of the Ti-DLC film as a function of the Ti concentration. The internal stress of the DLC films without Ti is up to ~0.9 GPa. As the Ti concentration is 0.21 at.%, the internal stress decreases dramatically from 0.9 GPa to 0.3 GPa. The Ti concentration increases further, the internal stress keeps constant value of 0.31 ± 0.01 GPa. The most important three factors of the stress reduction should be considered here. First, the decrease of the internal stress could be assigned to the increase of the sp^2-C fraction because of the Ti atom doping (as shown in Fig. 4) [28,29]. Second, the increase of the adatom mobility induced by Ti$^+$ ions bombardment probably relaxes the internal stress [30]. At last, at a low doping level, the incorporated metal atom plays a role of a pivotal site, where the distortion of the atomic bond angles can occur, which causes the significant reduction of the internal stress. However, the hardness of the films keeps at a constant value (10 ± 1 GPa) after the incorporation of different low concentration Ti, which may attribute to the relatively constant sp^3/sp^2 ratio (0.37 ± 0.04) in the films. It must be noted that the hardness could keep at a high level (~10 GPa), although the internal stress exhibited a significant reduction as long as the Ti is at low concentration doping level. Meanwhile, at a low concentration
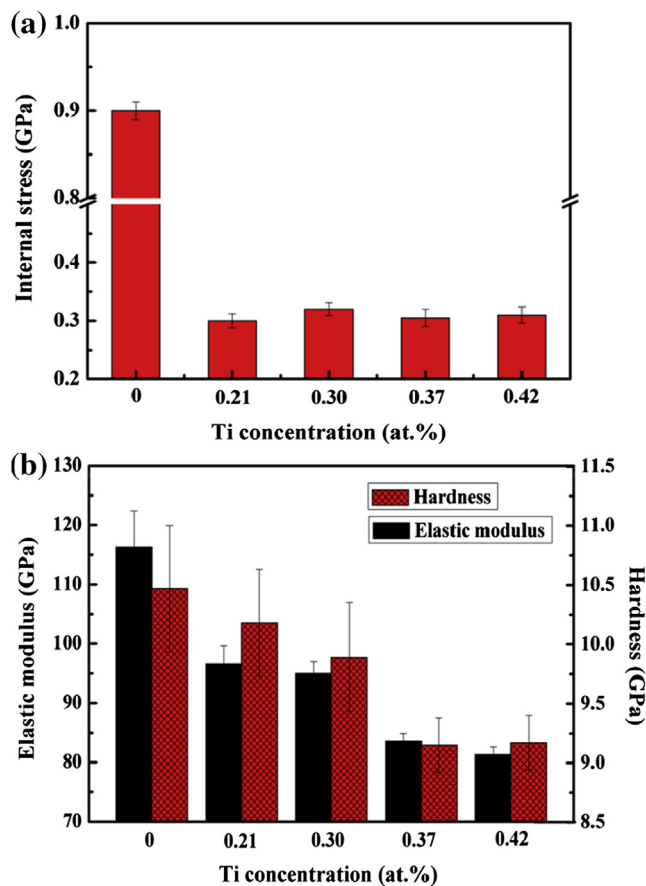
doping level, the microstructure and properties of the films almost could not be impacted as the change of the doped Ti concentration.

3.5. Tribological properties

Fig. 6 shows the friction coefficient curves of the films as a function of sliding distance and wear rate of the films with the different Ti concentration. All the low concentration Ti-doped DLC films show lower friction coefficient compared with the pure DLC film. Furthermore, the severely fluctuating friction coefficient curve could be observed for the pure DLC film, and the film fails after 50 min sliding with a higher friction coefficient (~0.1), while the low concentration Ti-doped DLC films are able to keep the stable friction coefficient of around 0.04 without failure even after 120 min, which indicates low concentration Ti doping could effectively reduces the friction coefficient of the DLC film. Moreover, the wear rate of the pure DLC film is kept at relatively high value of 6.2×10^{-6} mm^3/Nm. When the Ti concentration is 0.21 at.%, the wear rate decreases to lower value of 2.4×10^{-8} mm^3/Nm, almost 3 times lower than the pure DLC film. As the Ti concentration increases further, the wear rate has almost no obvious change. Above results demonstrated clearly that the introduction of low concentration Ti decreases the friction coefficient and wear rate of the DLC film and no obvious difference is observed at different Ti concentration, probably due to the narrow difference in Ti concentration.
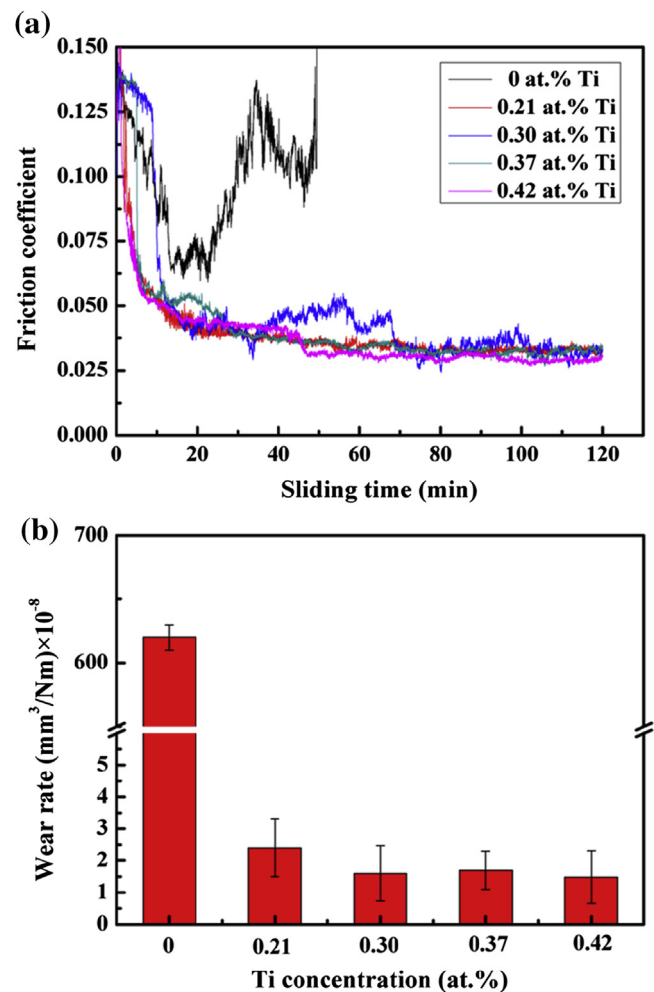

Fig. 5. (a) Internal stress (b) hardness, elastic modulus of the Ti-DLC films as a function of the Ti concentration.

Fig. 6. (a) Friction coefficient of the films as a function of sliding distance (b) wear rate of the films with the different Ti concentration.
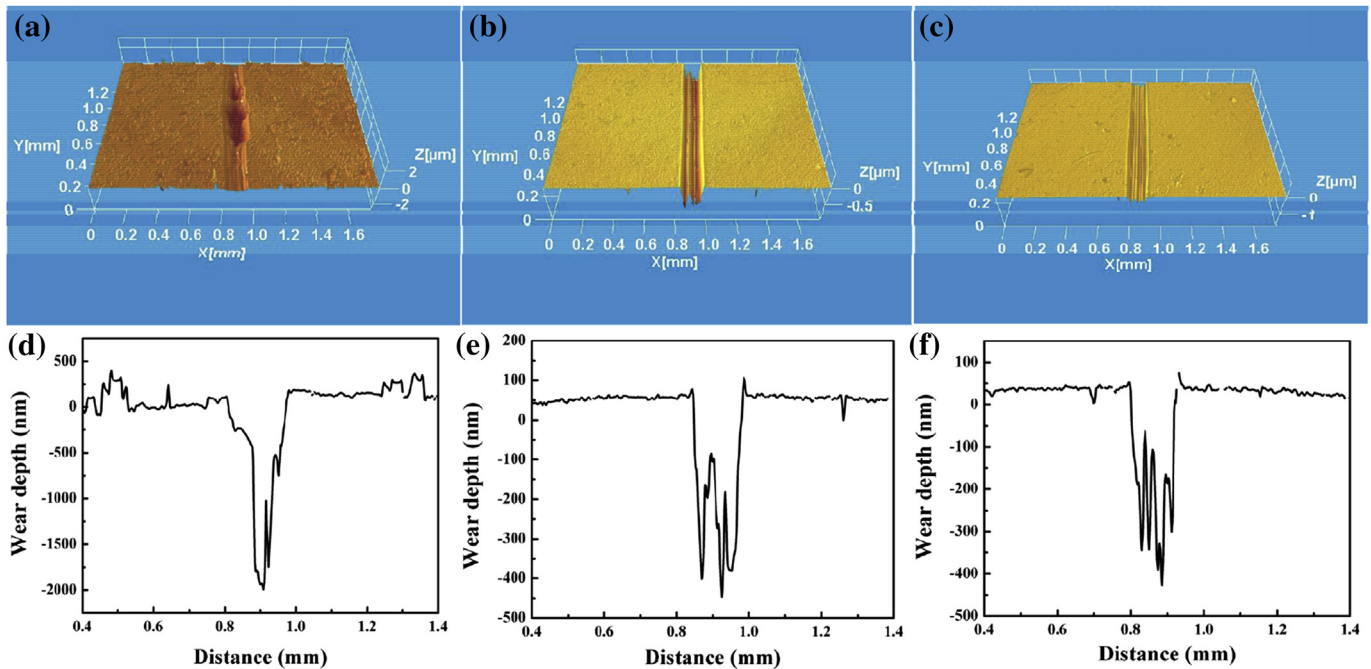
Fig. 7. The 3D images and corresponding 2D cross-section profiles of wear tracks of the films with the Ti concentration of (a and d) 0, (b and e) 0.21, (c and f) 0.42 at.%.

Fig. 7 shows the 3D images and corresponding 2D cross-section profiles of wear tracks of the films with the Ti concentration of the 0, 0.21 and 0.42 at.%, respectively. Obviously, the pure DLC film presents more serious wear than the other low concentration Ti-doped DLC films, and an obvious groove can be observed in Fig. 7(a), while the other Ti-DLC films exhibit a smaller wear scar compared with the pure DLC film, and similar wear scar at a low concentration Ti doping level. Moreover, the pure DLC film presents deep and broad wear tracks, while the wear tracks of the Ti-doped DLC films are shallow and narrow, which demonstrates that the low concentration Ti-doped DLC film improved the wear resistance of DLC film significantly, which is attributed to the combined protection of relatively high hardness and low stress.

4. Conclusions

Different low concentration Ti-doped DLC films were prepared using a magnetron sputtering Ti twin-targets in the methane and argon mixture atmosphere by varying the Ar/CH_4 flow ratio. In the low concentration (<0.42 at.%) range, no Ti−C bonds are observed in the films, and the sp^2/sp^3 ratio almost keeps constant without any obvious change. The hardness decreases slightly with the increase of Ar/CH_4 flow ratio, but it still retains at high level (∼10 GPa), which is mainly assigned to the relatively stable sp^2/sp^3 ratio; while the internal stress exhibits a significant reduction compared with the pure DLC film. Furthermore, the Ti-DLC films with low concentration Ti doping show good tribological properties with a wear rate of $2.0 \pm 0.2 \times 10^{-8}$ mm^3/Nm and a low friction coefficient of about 0.04, which implies the DLC film has excellent performance, and it could not have any changes with the change of the Ti content as long as the amount of Ti doping in the low content level.

Acknowledgments

References

[1] J. Robertson, Diamond-like amorphous carbon, Materials Science and Engineering: R: Reports 37 (2002) 129.
[2] Z. Wang, C.B. Wang, B. Zhang, Q. Wang, J.Y. Zhang, Effect of negative bias on the structure, topological and tribological properties of amorphous carbon films prepared by magnetron sputtering, Surface and Interface Analysis 43 (2011) 1218−1223.
[3] G. Cho, B.K. Yen, C.A. Klug, Structural characterization of sputtered hydrogenated amorphous carbon films by solid state nuclear magnetic resonance, Journal of Applied Physics 104 (2008) 013531.
[4] X.L. Bui, Y.T. Pei, J.T.M. De Hosson, Magnetron reactively sputtered Ti-DLC coatings on HNBR rubber: the influence of substrate bias, Surface & Coatings Technology 202 (2008) 4939−4944.
[5] H.Y. Dai, H. Jiang, C.Y. Zhan, N.K. Huang, Effects of sputtering current on the bonding structure and mechanical properties of diamond-like carbon films deposited by MFPUMST, Surface and Interface Analysis 41 (2009) 560.
[6] J. Zhu, J. Han, X. Han, H.I. Schlaberg, J. Wang, sp^3-rich deposition conditions and growth mechanism of tetrahedral amorphous carbon films deposited using filtered arc, Journal of Applied Physics 104 (2008) 013512.
[7] M.C. Kang, H.S. Tak, Y.K. Jeong, H.W. Lee, J.S. Kim, Properties and tool performance of ta-C films deposited by double-bend filtered cathodic vacuum arc for micro drilling applications, Diamond & Related Materials 19 (2010) 866−869.
[8] J.V. Rau, R. Teghil, A. De Bonis, A. Generosi, B. Paci, R. Generosi, M. Fosca, D. Ferro, V. Rossi Albertini, N.S. Chilingarov, Pulsed laser deposition of hard and superhard carbon thin films from C_{60} targets, Diamond & Related Materials 19 (2010) 7−14.
[9] B. Racine, M. Benlahsen, K. Zellama, R. Bouzerar, J.P. Kleider, H.J. Von Bardeleben, Electronic properties of hydrogenated amorphous carbon films deposited using ECR-RF plasma method, Diamond & Related Materials 10 (2001) 200−206.
[10] S.F. Yoon, K.H. Tan, Rusli, J. Ahn, Q.F. Huang, Comparative study on the effects of ion density and ion energy on diamond-like carbon deposited by electron cyclotron resonance chemical vapor deposition, Journal of Applied Physics 89 (2001) 4830−4835.
[11] B. Yang, Z.H. Huang, C.S. Liu, Z.Y. Zeng, X.J. Fan, D.J. Fu, Characterization and properties of Ti-containing amorphous carbon nanocomposite coatings prepared by middle frequency magnetron sputtering, Surface & Coatings Technology 200 (2006) 5812−5818.
[12] F. Zhao, H.X. Li, L. Ji, Y.J. Wang, H.D. Zhou, J.M. Chen, Ti-DLC films with superior friction performance, Diamond & Related Materials 19 (2010) 342−349.
[13] V. Singh, J.C. Jiang, E.I. Meletis, Cr-diamond like carbon nanocomposite films: synthesis, characterization and properties, Thin Solid Films 489 (2005) 150−158.

[14] G.A. Zhang, P.X. Yan, P. Wang, Y.M. Chen, J. Zhang, L.P. Wang, J.Y. Zhang, The effect of applied substrate negative bias voltage on the structure and properties of Al-containing a-C: H thin films, Surface & Coatings Technology 202 (2008) 2684—2689.

[15] J. Veverkova, S.V. Hainsworth, Effect of temperature and counterface on the tribological performance of W-DLC on a steel substrate, Wear 264 (2008) 518—525.

[16] K.D. Ma, G.B. Yang, L.G. Yu, P.Y. Zhang, Synthesis and characterization of nickel-doped diamond-like carbon film electrodeposited at a low voltage, Surface & Coatings Technology 204 (2010) 2546—2550.

[17] P.V. Bharathy, D. Nataraj, P.K. Chu, H.Y. Wang, Q. Yang, M.S.R.N. Kiran, J. Silvestre-Albero, D. Mangalaraj, Effect of titanium incorporation on the structural, mechanical and biocompatible properties of DLC thin films prepared by reactive-biased target ion beam deposition method, Applied Surface Science 257 (2010) 143—150.

[18] K. Bewilogua, R. Wittorf, H. Thomsen, M. Weber, DLC based coatings prepared by reactive d. c. magnetron, Thin Solid Films 447—448 (2004) 142—147.

[19] W. Dai, P.L. Ke, A.Y. Wang, Microstructure and property evolution of Cr-DLC films with different Cr content deposited by a hybrid beam technique, Vacuum 85 (2011) 792—797.

[20] W. Dai, A.Y. Wang, Deposition and properties of Al-containing diamond-like carbon films by a hybrid ion beam sources, Journal of Alloys and Compounds 509 (2011) 4626—4631.

[21] I. Gerhads, C. Roning, U. Vetter, H. Hofsass, G. Gibhardt, G. Eckold, Q. Li, S.T. Lee, Y.L. Huang, M. Seibt, Ion beam synthesis of amorphous carbon thin films containing metallic nanoclusters, Surface & Coatings Technology 158—159 (2002) 114—119.

[22] A.T.T. Koh, J. Hsieh, D.H.C. Chua, Structural characterization of dual-metal containing diamond-like carbon nanocomposite films by pulsed laser deposition, Diamond & Related Materials 29 (2010) 637—642.

[23] P.C. Tsai, J.Y. Chiang, Y.F. Hwang, Characteristics and mechanical properties of titanium-containing diamond like carbon films deposited by cathodic arc evaporation, Journal of Nanoscience and Nanotechnology 8 (2008) 2516—2521.

[24] J.F. Cui, L. Qiang, B. Zhang, X. Ling, T. Yang, J.Y. Zhang, Mechanical and tribological properties of Ti-DLC films with different Ti content by magnetron sputtering technique, Applied Surface Science 258 (2012) 5025—5030.

[25] P. Wang, X. Wang, Y.M. Chen, G.A. Zhang, W.M. Liu, J.Y. Zhang, The effect of applied negative bias voltage on the structure of Ti-doped a-C: H films deposited by FCVA, Applied Surface Science 253 (2007) 3722—3726.

[26] P.L. Wong, F. He, X. Zhou, Interpretation of the hardness of worn DLC particles using micro-Raman spectroscopy, Tribology International 43 (2010) 1806—1810.

[27] N. Paik, Raman and XPS studies of DLC films prepared by a magnetron sputter-type negative ion source, Surface & Coatings Technology 200 (2005) 2170—2174.

[28] Y.B. Zhang, S.P. Lau, D. Sheeja, B.K. Tay, Study of mechanical properties and stress of tetrahedral amorphous carbon films prepared by pulse biasing, Surface & Coatings Technology 195 (2005) 338.

[29] G. Capote, F.L. Freire, L.G. Jacobsohn, G. Mariotto, Amorphous hydrogenated carbon films deposited by PECVD in methane atmospheres highly diluted in argon: effect of the substrate temperature, Diamond & Related Materials 13 (2004) 1454—1458.

[30] Y.N. Kok, P.E. Hovsepian, Q. Luo, D.B. Lewis, J.G. Wen, I. Petrov, Influence of the bias voltage on the structure and the tribological performance of nanoscale multilayer C/Cr PVD coatings, Thin Solid Films 475 (2005) 219—226.